Research Article

iMedPub Journals
http://www.imedpub.com/

Journal of Anatomical Science and Research

2018
Vol.1 No.2:4

Myosin Heavy Chain Expression in the External Urethral Sphincter of Rats with Simulated Birth Trauma

Toshiko Tsumori[1*] and Wakako Tsumiyama[2]

[1]Department of Nursing, Faculty of Health and Welfare, Prefectural University of Hiroshima, Mihara, Japan

[2]Department of Physical Therapy, Faculty of Health and Welfare, Prefectural University of Hiroshima, Mihara, Japan

[*]**Corresponding author:** Toshiko Tsumori, Department of Nursing, Faculty of Health and Welfare Prefectural University of Hiroshima, 1-1 Gakuen-cho, Mihara City, Hiroshima Prefecture 723-0053, Japan Tel: +81-848-60-1222; Fax: +81-848-60-1134; E-mail: t-tsumori@pu-hiroshima.ac.jp

Received date: June 28, 2018; **Accepted date:** July 23, 2018; **Published date:** July 27, 2018

Citation: Tsumori T, Tsumiyama W (2018) Myosin Heavy Chain Expression in the External Urethral Sphincter of Rats with Simulated Birth Trauma. J Anat Sci Res Vol. 1 No.2: 4

Abstract

Objective: Various animal models have been developed to understand the pathophysiology of stress urinary incontinence and identify suitable therapies. One of the most common animal models, a vaginal distention model that simulates the second phase of labor, has been shown to damage the pelvic floor muscles, particularly the external urethral sphincter, in rats and mice. The external urethral sphincter plays a crucial role in urinary continence. This study aimed to examine the changes in the fiber-type composition of this skeletal sphincter muscle under pathophysiological conditions in order to evaluate its functional and metabolic properties.

Methods: We used triple immunofluorescence labeling to visualize one slow (type 1) and two fast (types 2A and 2B) myosin isoforms in the female rat external urethral sphincter and examined changes in their expression within the sphincter 4 weeks after vaginal distention in an established animal model of postpartum stress urinary incontinence.

Results: We found that the fiber-type compositions were similar to those of intact animals, with type 2A fibers predominant throughout the sphincter, and type 2B fibers restricted to the proximal segment. Type 1 fibers were concentrated in the proximal and distal ends of the sphincter. However, the ratio of total cross-sectional area of type 2B fibers was significantly reduced in rats with vaginal distention. Moreover, the minor diameter of type 2B fibers was significantly decreased.

Conclusion: These findings indicate that vaginal distention may induce irreversible changes in myosin heavy chain expression in the rat external urethral sphincter, especially of type 2B isoforms.

Keywords: External urethral sphincter; Myosin heavy chain; Type 2B fibers; Vaginal distention; Stress urinary incontinence; Immunofluorescence; Rat

Introduction

Stress urinary incontinence (SUI) in women is known to be caused by pregnancy, delivery, obesity, and aging. The most common type of SUI is related to the trauma of vaginal childbirth [1]. SUI can seriously impact postpartum activity and quality of life in women. To better understand the pathophysiology of SUI, animal models have been developed to simulate various human situations [2-4]. One of the most common models is vaginal distention (VD), which was first developed by Lin et al. [5] in rats. VD simulates the second phase of labor and has been shown to damage the pelvic floor muscles, particularly the external urethral sphincter (EUS) and peripheral branches of the pudendal nerve [3,6]. Several modifications to the originally reported technique of inducing VD have been reported, including the size of the Foley catheter inserted into the rat vagina, balloon dilation volume, inflation time, and animals' age or reproductive stage [5,7-13]. Regardless of such variations in methodology, VD damages urethral function in the short term and reduces urethral resistance to leakage, resulting in SUI that recovers with time [4].

The EUS is a unique striated muscle tissue that encloses the urethra [14,15], and it plays a critical role in urethral closure mechanisms during urinary continence [16,17]. Establishing a full understanding of the anatomical and physiological features of the EUS is essential to understanding the pathophysiology of SUI. Myosin heavy chain (MHC) isoforms are the most appropriate markers for delineating the fiber types in skeletal muscle [18]. Our recent study demonstrated that the rat EUS of both sexes expressed three MHC isoforms, one slow (type 1) and two fast (types 2A and 2B), using triple immunofluorescence labeling [19]. We observed a clear sexual dimorphism and regional differences in the fiber-type composition of the rat EUS along the longitudinal axis of the urethra. A detailed knowledge of changes in the fiber-type composition of the EUS in the presence of pathophysiological conditions is essential to evaluating its functional and metabolic properties.

VD has been recognized as an animal model of myogenic damage-related SUI [11]. Lin et al. [5] first demonstrated that

the urethral wall musculature, including both smooth and striated muscles, diminished in incontinent rats subjected to VD. VD caused severe disruption and marked thinning of the EUS [8]. The expression of caveolin-3 and neuronal nitric oxide synthase significantly decreased in the urethral striated muscle after VD [7]. Serum skeletal muscle enzymes such as lactose dehydrogenase and creatine kinase, which are indicators of increased muscle cell membrane permeability and skeletal muscle damage, increased and peaked on day 7 after VD [12]. Lin et al. [5] indicated that muscle necrosis and degeneration, irregular shape and size of muscle fibers, and a change in the ratio of type 1 and type 2 fibers were prominent features in the levator ani after VD, although they did not report the fiber-type changes in the EUS. Thus, to the best of our knowledge, no data are available concerning the changes in the fiber-type composition of the rat EUS after VD. Therefore, the aim of this study was to examine whether the MHC isoform expression patterns change in the EUS after VD using triple immunofluorescence labeling.

Materials and Methods

Animals

All of the experiments were approved by the Animal Care and Use Committee of the Prefectural University of Hiroshima. Eight-week-old female Wistar rats were purchased from Hiroshima Experimental Animals Co. (Hiroshima, Japan). A total of 12 animals were divided into two groups: 7 underwent VD and 5 served as intact controls. The animals in the VD group were anesthetized *via* intraperitoneal (IP) injection of medetomidine (0.3 mg/kg), midazolam (4.0 mg/kg), and butorphanol (5.0 mg/kg). According to the method described by Lin et al., a 12-Fr Foley catheter with the tip cut off was inserted into the vagina, and the balloon was inflated with 2 ml of water. The labia majora were sutured to prevent ejection of the dilated balloon. After 4 h, the balloon was deflated and removed from the vagina. The intact group received no such treatment. Both groups were housed with access to water and food ad libitum until they reached 12 weeks of age. Then, the animals were euthanized by an IP pentobarbital overdose (100 mg/kg).

Tissue preparation

After a ventral abdominal incision, the bladder and urethra were exposed by opening the pubic bone. The urethra was removed with the vagina from the meatus to the bladder neck. The specimens were embedded in optimal cutting temperature compound and frozen in liquid nitrogen. Serial 12 µm longitudinal sections were cut on a cryostat (HYRAX C 50; Carl Zeiss Microscopy GmbH, Jena, Germany). All of the collected sections contained EUS muscle fibers. Some sections were stained with hematoxylin-eosin to detect the architectural landmarks of the EUS and urethra.

Immunofluorescence labeling of MHC isoforms in the EUS

The sections were rinsed in 0.1 M phosphate-buffered saline (PBS) at pH 7.3 and incubated for 1 h at room temperature in PBS containing 0.2% Triton 100X, 1% bovine serum albumin (BSA), and 5% normal goat serum (NGS). The tissues were incubated overnight with the primary antibody cocktail at 4°C. The combination of the primary antibodies used to detect MHC isoform expression was similar to that used in a previous study [20] and consisted of mouse type 1 immunoglobulin (Ig) G2b (1: 100 dilution), type 2A IgG1 (1: 50 dilution), and type 2B IgM (1: 50 dilution) antibodies that were diluted in PBS containing 0.2% Triton 100X, 1% BSA, and 5% NGS. All of the primary antibodies were obtained from the Developmental Studies Hybridoma Bank (Iowa City, IA, USA). Following incubation with the primary antibodies, the sections were washed with PBS and incubated for 1–2 h at room temperature with the following secondary antibodies, which were diluted in PBS containing 0.2% Triton 100X, 1% BSA, and 5% NGS: Alexa Fluor® 350-conjugated goat anti-mouse IgG2b, (1: 500 dilution; Invitrogen, Carlsbad, CA, USA), Alexa Fluor® 594-conjugated goat anti-mouse IgG1 (1: 500 dilution, Invitrogen), and Alexa Fluor® 488-conjugated goat anti-mouse (1: 500 dilution, Invitrogen). The sections were subsequently washed in PBS and mounted in Vectashield™ Mounting Medium (Vector Laboratories, Burlingame, CA, USA). Negative control assays were performed that involved the same staining procedure in the absence of the primary antibodies, and positive signals were not detected in the tissues that had undergone these assays. Fluorescent images were acquired using a fluorescence microscope (BZ-X700; Keyence Corporation, Osaka, Japan).

Data analysis

We examined only the ventral wall of the EUS in the sagittal sections, because the distal segment of its dorsal wall was incomplete or missing, as described in our recent publication [19]. Images (100X) of the complete ventral wall in the proximal, middle, and distal segments of each animal were captured in the midsagittal plane of the urethra. The captured images were analyzed, and the cross-sectional areas (CSAs) of the positively labeled fiber types (1, 2A, and 2B) were calculated using the BZ-X700 analysis application (Keyence Corporation). The percentage of a fiber type in each segment of the EUS was calculated as the sum of the CSA of a fiber type divided by the total CSA of the three fiber types. In addition, higher-magnification images (400X) were obtained from midsagittal sections of the proximal segments of the EUS to measure the minor diameters of each fiber type. The data were statistically analyzed using the unpaired t-test or the Mann-Whitney U test, and expressed as means and standard errors of the mean or median (minimum-maximum), respectively. All statistical analyses were performed with SPSS Statistics software version 23 for Microsoft Windows (IBM Corp., Armonk, NY, USA).

Results

General appearance of the EUS stained with hematoxylin-eosin

The general structure of the female EUS was consistent with the observations described in our previous study [19]. Briefly, in the sagittal sections of the urethra, the EUS was apparent as the cross-sectional profiles of the striated muscle fibers embedded in the connective tissues of the urethral wall **(Figure 1).**

The EUS was thickest in the proximal segment at both the ventral and dorsal walls of the urethra, whereas its distal segment became thinner in the ventral wall and was missing from the dorsal wall. The EUS of rats that underwent VD appeared slightly thinner than those of intact animals, particularly in the proximal segment.

Moreover, higher-magnification images revealed that the muscle profile of rats subjected to VD contained fewer larger-sized fibers compared with that of intact animals **(Figure 1).** However, no pathological changes, i.e., muscle necrosis and degeneration, were observed in the EUS of rats that underwent VD.

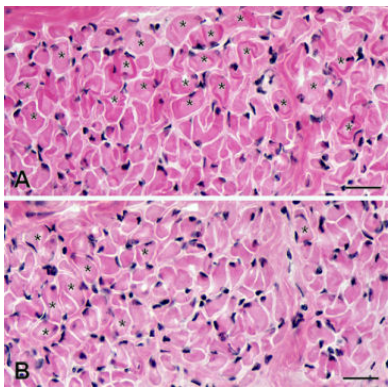

Figure 1: High-power views showing the proximal segment of the external urethral sphincter (EUS) in hematoxylin and eosin-stained sagittal sections of the urethra from an intact rat (A) and a rat that underwent VD (B). Note the cross-sectional profiles of the striated muscle fibers embedded in the connective tissue. Fiber profiles with a larger diameter, indicated by asterisks, are often seen near the adventitial (upper) side of the muscle layer in the intact rat (A) (scale bar: 20 µm), while these fiber profiles are rare in a rat that underwent VD (B) (scale bar: 50 µm).

MHC expression in the EUS using triple immunofluorescence labeling

As we reported in our recent study [19], triple immunofluorescence labeling clearly showed the distribution of types 1, 2A, and 2B fibers in the female rat EUS **(Figures 2 and 3).** The distribution patterns of each fiber type in every segment of the EUS are shown in **Figure 4**, which are consistent with our previous report [19].

In short, type 2A fibers were dominant throughout the EUS, while almost all of the type 2B fibers were localized to the proximal segment. Type 1 fibers were concentrated at both the proximal and distal ends **(Figure 4).**

However, the ratio of total CSA of type 2B fiber in the proximal segment was significantly decreased in rats that underwent VD compared to that in intact animals. The CSA of each fiber type in the three segments of the EUS is summarized in **Table 1**. In the EUS of rats that underwent VD, the CSA of type 2B fibers was significantly decreased compared with that of intact rats.

Figure 3 shows a representative animal from the VD group, in which the proximal segment of the EUS contained fewer type 2B fiber profiles. Conversely, the CSA of type 1 fibers in the EUS of rats that underwent VD was increased in all segments, although this difference reached statistical significance only in the middle segment.

The total CSA of the three types of fibers in the proximal segment of the EUS was significantly decreased in animals with VD compared with intact rats, although there was no significant difference between the intact and VD groups in either the middle or distal segments. The higher-magnification views revealed that type 2B fibers in the VD animals were markedly smaller than those in the intact animals **(Figure 5).**

A small proportion of type 1/2A hybrid fibers were detected in the EUS of both intact and VD animals **(Figure 6).**

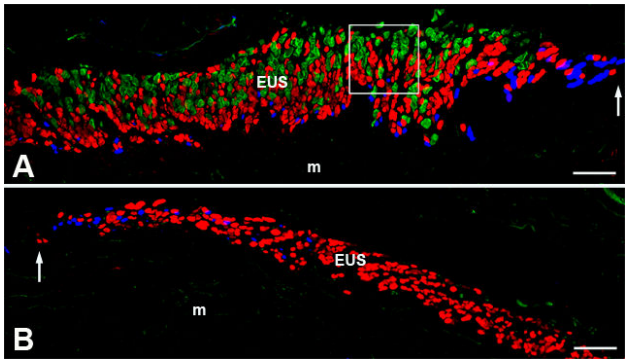

Figure 2: Fluorescence microscopy images showing the three myosin isoforms (type 1, blue; type 2A, red; and type 2B, green) in the external urethral sphincter (EUS) of an intact rat using a triple immunolabeling technique. A, B: Low-power view showing the proximal (A) and distal (B) segments of the ventral wall of the EUS (scale bars: 100 µm). The proximal segment contains three fiber types, namely, types 1, 2A, and 2B. Type 1 fibers are located in the adluminal region, while type 2B fibers are situated near the adventitial (upper) side of the muscle layer. A boxed area in A is enlarged in **Figure 5A.** The distal segment predominantly contains type 2A fibers and a lesser number of type 1 fibers, with no type 2B fibers. Arrows indicate the proximal end (A) and the distal end (B) of the EUS (m, urethral mucosa).

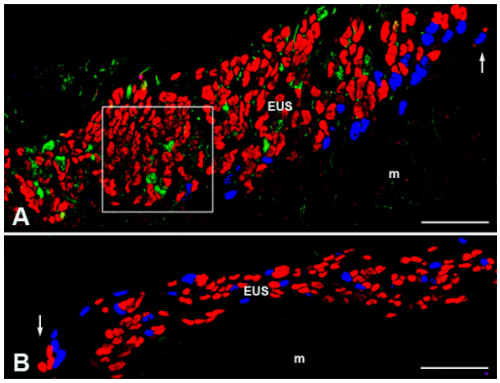

Figure 3: Fluorescence microscopy images showing the three myosin isoforms (type 1, blue; type 2A, red; and type 2B, green) in the external urethral sphincter (EUS) from a rat that underwent VD using a triple immunolabeling technique. A, B: A representative case showing the proximal (A) and distal (B) segments of the ventral wall of the EUS (scale bars: 100 µm). Type 2A fibers are predominant throughout both segments, and type 1 fibers are concentrated at both ends. In this case, the proximal segment contains few type 2B fiber profiles. A boxed area in A is enlarged in **Figure 5B**. Arrows indicate the proximal end (A) and the distal end (B) of the EUS (m, urethral mucosa).

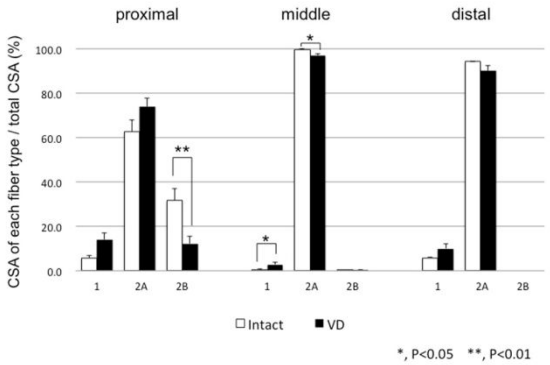

Figure 4: Distribution of the three fiber types in each segment of the external urethral sphincter (EUS) in an intact rat and a rat that underwent VD. Type 2A fibers predominate throughout the EUS, while type 2B fibers are restricted to the proximal segment. The ratio of type 2B fibers in rats that underwent VD is significantly lower than that in intact animals. $^{*}P < 0.05$; $^{**}P < 0.01$.

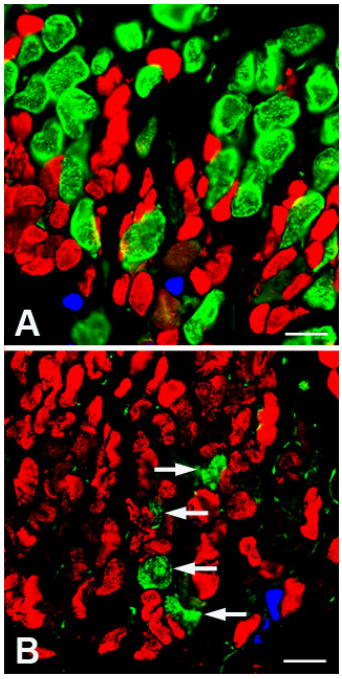

Figure 5: Fluorescence microscopy images showing the three myosin isoforms (type 1, blue; type 2A, red; and type 2B, green) in the external urethral sphincter (EUS) using a triple immunolabeling technique. A, B: Enlarged views of the boxed areas in **Figures 2** (an intact rat) **and 3** (a representative animal that underwent VD), respectively (scale bars: 20 µm). Type 2B fibers are the largest among the three fiber types of the intact rat (A), while their profiles are smaller (arrows) in a rat that underwent VD (B).

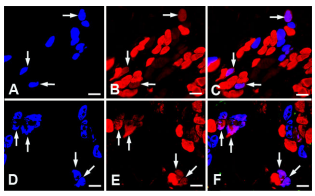

Figure 6: Fluorescence microscopy images showing the presence of type 1/2A hybrid fibers in the proximal segment of the external urethral sphincter (EUS) in an intact rat (A-C) and a representative animal that underwent VD (D-F). A–C: Examples of type 1/2A hybrid fibers (arrowheads). A, D: Type 1; B, E: type 2A; and C, F: a merged view incorporating panels A and B or D and E (scale bar: 20 µm).

The average minor diameters of each fiber type in the proximal segment of the EUS in intact and VD animals are summarized in **Table 2.** In general, type 1 fibers were the smallest, and type 2B fibers were the largest in both groups. Both type 2A and 2B fibers were significantly smaller in rats that underwent VD than in intact animals. By contrast, type 1 and type 1/2A hybrid fibers were significantly larger in rats that underwent VD than in intact animals.

Table 1: Comparison of the cross-sectional areas of the fiber types in each segment of the external urethral sphincter between the intact and VD groups.

Segment	Fiber type	Intact ($x10^2$ μm^2)	VD ($x10^2$ μm^2)
	Type 1	53.2 ± 11.5	91.2 ± 17.8
	Type 2A	553.2 ± 37.4	483.0 ± 31.8
	Type 2B	298.5 ± 65.0*	84.0 ± 25.8*
Proximal	Total	904.9 ± 86.8*	658.3 ± 33.7*
	Type 1	1.3 ± 0.8*	11.4 ± 3.4*
	Type 2A	344.5 ± 71.7	360.2 ± 42.7
	Type 2B	0.0 (0.0 -2.6)	0.0 (0.0 -2.6)
Middle	Total	346.3 ± 72.6	372.2 ± 45.0
	Type 1	27.4 ± 1.5	39.4 ± 9.9
	Type 2A	433.5 (356.2-519.2)	288.6 (283.5 -468.5)
	Type 2B	0	0
Distal	Total	462.5 (379.1-551.3)	324.2 (299.9-537.7)

Values presented are the means ± the standard errors of the means or the median (minimum-maximum). *P<0.05 indicates a statistically significant difference compared with the intact group using the unpaired t-test or Mann-Whitney U test. Intact, N=5; VD, N=7.

Table 2: Comparison of the average minor diameter of each fiber type in the proximal segment of the EUS between the intact and VD groups.

Fiber type	Intact (μm)	VD (μm)
Type 1	8.0 ± 0.1 (n=200)	8.6 ± 0.1** (n=310)
Type 1/2A	6.7 ± 0.4 (n=10)	9.5 ± 0.6** (n=26)
Type 2A	9.1 ± 0.1 (n=487)	8.5 ± 0.1** (n=819)
Type 2B	13.3 ± 0.1 (n=542)	10.9 ± 0.2** (n=184)

Values are presented as the mean ± standard error of the mean. **P<0.01 indicates a statistically significant difference compared with the intact group using the unpaired t-test or Mann-Whitney U test. Intact, N=5; VD, N=7.

Discussion

The present study used triple immunofluorescence labeling to investigate MHC isoform expression in the female rat EUS 4 weeks after VD. We demonstrated that the distribution pattern of fiber types in the EUS did not differ between the intact and VD groups: type 2A fibers were dominant throughout the EUS, while almost all type 2B fibers were localized to the proximal segment, and type 1 fibers were concentrated at the proximal and distal ends. However, the fiber-type composition in the proximal segment differed markedly between the intact and VD groups. The ratio of total CSA of type 2B fibers significantly decreased in the proximal segment of the EUS after VD. Moreover, not only type 2B fibers but also type 2A fibers were significantly reduced in size. Conversely, type 1 and type 1/2A hybrid fibers were larger in the EUS after VD.

The VD model has been applied in the evaluation of myogenic damage and recovery [11]. Using a VD mouse model, Lin et al. [20] demonstrated that leak point pressure was recovered 20 days after VD, and this recovery was associated with repair of the EUS. Huang et al. [12] found that lactose dehydrogenase and creatine kinase, serum biochemical markers indicating muscle injury, peaked on day 7 and gradually declined, returning to near-normal levels 28 days after VD. In the present study, we employed the original VD model described by Lin et al. [5] to simulate birth trauma, and we immunohistochemically examined MHC expression in the EUS 4 weeks (28 days) after VD, which, based on previous experiments [12,21], appears to be a sufficient period for functional recovery from the muscle injury. Nonetheless, we found that the fiber-type composition in the proximal segment of the EUS 4 weeks after VD differed from that of intact animals in that the proportion of type 2B fibers was significantly lower. Thus, the morphological evidence obtained in the current study may not corroborate previous

pathophysiological data. In both our previous and present studies, type 2B fibers were observed only in the proximal segment of the female rat EUS, suggesting that this segment of the EUS plays an important role in coordination with the bladder neck during micturition and/or continence. Buffini et al. [21] suggested that type 2B fibers in the female rat EUS are small, oxidative, and resistant to fatigue, which differs from typical type 2B fibers that are large, glycolytic, and easily fatigable. Therefore, it is reasonable to consider that a reduced number and/or atrophy of the type 2B fibers in the proximal segment of the EUS could directly influence its contractile property in response to rapid changes in abdominal pressure. Moreover, not only type 2B fibers but also type 2A fibers, which occupied a larger portion of the female rat EUS, demonstrated atrophy. These findings are consistent with the result described by Lin et al. [5], indicating that the ratio of type 2 fiber decreased in the levator ani of incontinent rats 4 weeks after VD. Further studies are necessary to investigate whether the fiber-type composition and/or areal density of the fiber types present in the rat EUS is ultimately restored after VD, or whether VD leads to irreversible changes in MHC expression in the rat EUS, particularly of the type 2B isoform.

Ischemia-reperfusion injury can lead to urinary incontinence, simulating the childbirth-related injuries seen in postpartum SUI [22]. A prolonged second stage of labor has been reported to result in pressure-induced ischemia to the urethral skeletal muscle [23]. Damaser et al. [9] demonstrated that VD results in decreased blood flow to, and consequently hypoxia of, the bladder, urethra, and vagina, suggesting that hypoxic injury is a possible mechanism of injury leading to SUI. VD simulates prolonged second-stage labor and prolonged mechanical compression of the pelvic floor, resulting in tissue hypoxia from decreased blood flow to the pelvic organs [12]. Cannon et al. [8] demonstrated that rats subjected to prolonged VD had the greatest histological evidence of urethral damage, especially to the skeletal muscle layer. They concluded that pressure-induced ischemia caused pelvic floor injury and dysfunction of the urethral continence mechanism. The present study is the first to demonstrate that VD induces changes in the fiber-type composition and the size of fibers present in the EUS. Notably, such changes occurred mainly in the type 2B fibers in the EUS. Chan et al. [24] suggested that skeletal muscle reperfusion injury predominantly affects type 2 fibers with low myosin content. Hence, it is possible that VD-induced ischemia following hypoxia and/or reperfusion resulted in injuries to fast-twitch fibers, particularly type 2B fibers, in the female rat EUS.

In contrast to type 2B fibers, we observed that the CSA of type 1 fibers in the EUS of rats subjected to VD was increased in all segments, a difference that was only significant in the middle segment. We also observed hypertrophy in a substantial number of type 1/2A hybrid fibers. Aging and/or gonadectomy has been reported to affect the fiber-type composition of the EUS in rabbits, dogs, and rats [19,25,26]. In a previous report, we demonstrated that the proportion of type 1 fibers increased in the EUS of ovariectomized rats. Under certain conditions, such as neuromuscular activity, mechanical loading or unloading, changes in hormone levels, and aging, transitions of MHC isoform expression in the skeletal muscles can occur, in either a fast-to-slow or slow-to-fast direction [18]. Changes to MHC isoform expression in the EUS may affect the contractile properties of this striated sphincter. However, the functional significance of the increase in the proportion of type 1 fibers and the appearance of hypertrophy in type 1 and type 1/2A hybrid fibers after VD remains unclear.

The fiber-type composition of the human EUS is still controversial. Early enzyme-based analyses demonstrated that the human EUS contained type 1 or both type 1 and 2 fibers, with age- and sex-related variation [27-30]. Fast-twitch type 2 muscle fibers in the levator ani were decreased in biopsy samples from women with SUI [31]. It is possible that women experience similar changes in the fiber-type composition of the EUS after childbirth to those observed in animals that undergo VD. However, pathological changes in the human EUS have not been reported due to the limited availability of urethral biopsy specimens from women with SUI.

Antepartum and/or postpartum pelvic floor exercises are regarded as the primary treatment of SUI [32]. Postpartum exercises, when performed with a vaginal device providing resistance or feedback, appear to decrease postpartum urinary incontinence, although some training using a conservative model was shown to be ineffective in preventing postpartum urinary incontinence [33]. Jiang et al. [34] concluded that the pelvic floor muscles (iliococcygeus and pubococcygeus muscles), unlike the EUS, do not contribute to the bladder-to-urethra continence reflex in rats, due to the absence of a functional branch from the pudendal nerve innervating the pelvic floor muscles. Therefore, efforts to develop effective exercise interventions to reduce postpartum urinary incontinence should focus on targeting organs and tissues that are specifically impaired in SUI. The present study indicated that VD led to possibly irreversible damage to type 2B fibers in the EUS. This finding may in turn suggest that vaginal birth trauma could induce an irreversible change in the composition of fast-twitch and slow-twitch fibers within the human EUS, which might lead to sphincter dysfunction. From this point of view, a novel intervention such as stem cell therapy may serve as an effective treatment for SUI [35].

In conclusion, we examined the expression pattern of MHC isoforms in the EUS of rats that underwent VD using triple immunofluorescence staining. We confirmed that the ratio of type 2B fibers decreased significantly in the proximal segment of the EUS, along with prominent atrophy of this fiber type, 4 weeks after VD. This finding suggests that VD may induce irreversible changes in MHC expression in the rat EUS, particularly of type 2B fibers. The female rat urethra shows a structural complexity consisting of the complicated mucosal foldings, longitudinal and circular smooth muscle layers, a striated muscle layer (EUS), and the submucosal venous plexus, all of which may be involved in the urethral continence mechanism [36]. However, this study was limited to the immunohistochemical analysis of MHC expression in the EUS 4 weeks after VD. Thus, future studies should investigate pathological changes in each type of fiber in the rat EUS after VD in a time-dependent manner and confirm whether those pathological changes are ultimately restored or not. Taken

together, these morphological approaches could be useful in the assessment of muscle injuries after VD in rat models of SUI and for the development of suitable antepartum and/or postpartum exercises or therapies to prevent urinary incontinence in women.

Conflict of Interest

No

Acknowledgement

This study was supported by JSPS KAKENHI (Grant-in-Aid for Scientific Research (C) 17K01523).

References

1. Fritel X, Ringa V, Quiboeuf E, Fauconnier A (2012) Female urinary incontinence, from pregnancy to menopause: A review of epidemiological and pathophysiological findings. Acta Obstet Gynecol Scand 91: 901-910.
2. Hijaz A, Daneshgari F, Sievert KD, Damaser MS (2008) Animal models of female stress urinary incontinence. J Urol 179: 2103-2110.
3. Gill BC, Moore C, Damaser MS (2010) Postpartum stress urinary incontinence: Lessons from animal models. Expert Rev Obstet Gynecol 5: 567-580.
4. Jiang HH, Damaser MS (2011) Animal models of stress urinary incontinence. Handb Exp Pharmacol 202: 45-67.
5. Lin AS, Carrier S, Morgan DM, Lue TF (1998) Effect of simulated birth trauma on the urinary continence mechanism in the rat. Urology 52: 143-151.
6. Sajadi KP, Gill BC, Damaser MS (2010) Neurogenic aspects of stress urinary incontinence. Curr Opin Obstet Gynecol 22: 425-429.
7. Sievert KD, Bakircioglu ME, Tsai T, Dahms SE, Nunes L, et al. (2001) The effect of simulated birth trauma and/or ovariectomy on rodent continence mechanism. Part 1: functional and structural change. J Urol 166: 311-317.
8. Cannon TW, Wojcik EM, Ferguson CL, Saraga S, Thomas C, et al. (2002) Effects of vaginal distension on urethral anatomy and function. BJU Int 90: 403-407.
9. Damaser MS, Whitebeck C, Chichester P, Levin RM (2005) Effect of vaginal distention on blood flow and hypoxia of urogenital organs of the female rat. J Appl Physiol 98: 1884-1890.
10. Pan HQ, Kerns JM, Lin DL, Liu S, Esparza N, et al. (2007) Increased duration of simulated childbirth injuries results in increased time to recovery. Am J Physiol Regul Integr Comp Physiol 292: R1738-R1744.
11. Hong SH, Piao S, Kim IG, Lee JY, Cho HJ, et al. (2013) Comparison of three types of stress urinary incontinence rat models: Electrocauterization, pudendal denervation, and vaginal distension. Urology 81: 465e1-465e6.
12. Huang J, Cheng M, Ding Y, Chen L, Hua K (2013) Modified vaginal dilation rat model for postpartum stress urinary incontinence. J Obstet Gynaecol Res 39: 256-263.
13. Song QX, Balog BM, Kerns J, Lin DL, Sun Y, et al. (2015) Long-term effects of simulated childbirth injury on function and innervation of the urethra. Neurourol Urodyn 31: 381-386.
14. Oelrich TM (1980) The urethral sphincter muscle in the male. Am J Anat 158: 229-246.
15. Oelrich TM (1983) The striated urogenital sphincter muscle in the female. Anat Rec 205: 223-232.
16. Ashton-Miller JA, Howard D, DeLancey JOL (2001) The functional anatomy of the female pelvic floor and stress continence control system. Scand J Urol Nephrol Suppl 207: 1-125.
17. Jung J, Ahn HK, Huh Y (2012) Clinical and functional anatomy of the urethral sphincter. Int Neurourol J 16: 102-106.
18. Pette D, Staron RS (2000) Myosin isoforms, muscle fiber types, and transitions. Microsc Res Tech 50: 500-509.
19. Tsumori T, Tsumiyama W (2017) Sexual and regional differences in myosin heavy chain expression in the rat external urethral sphincter. Anat Rec 300: 2058-2069.
20. Lin YH, Liu G, Li M, Xiao N, Daneshgari F (2010) Recovery of continence function following simulated birth trauma involves repair of muscle and nerves in the urethra in the female mouse. Eur Urol 57: 506-512.
21. Buffini M, O'Halloran KD, O'Herlihy C, O'Connell R, Jones JF (2010) Comparison of the contractile properties, oxidative capacities and fibre type profiles of the voluntary sphincters of continence in the rat. J Anat 217: 187-195.
22. Viktrup L, Rortveit G, Lose G (2008) Does the impact of subsequent incontinence risk factors depend on continence status during the first pregnancy or the postpartum period 12 years before? A cohort study in 232 primiparous women. Am J Obstet Gynecol 199: 73e1-73e4.
23. Handa VL, Garris TA, Ostergard DR (1996) Protecting the pelvic floor: Obstetric management to prevent incontinence and pelvic organ prolapse. Obstet Gynecol 88: 470-478.
24. Chan RK, Austen Jr WG, Ibrahim S, Ding GY, Verna N, et al. (2004) Reperfusion injury to skeletal muscle affects primarily type II muscle fibers. J Surg Res 122: 54-60.
25. Tokunaka S, Fujii H, Hashimoto H, Yachiku S (1993) Proportions of fiber types in the external urethral sphincter of young nulliparous and old multiparous rabbits. Urol Res 21: 121-124.
26. Augsburger HR, Cruz-Orive LM (1998) Influence of ovariectomy on the canine striated external urethral sphincter (M. urethralis): A stereological analysis of slow and fast twitch fibres. Urol Res 26: 417-422.
27. Gosling JA, Dixon JS, Critchley HO, Thompson SA (1981) A comparative study of the human external sphincter and periurethral levator ani muscles. Br J Urol 53: 35-41.
28. Schrøder HD, Reske-Nielsen E (1983) Fiber types in the striated urethral and anal sphincters. Acta Neuropathol (Berl) 60: 278-282.
29. Tokunaka S, Murakami U, Fujii H, Okamura K, Miyata M, et al. (1987) Coexistence of fast and slow myosin isozymes in human external urethral sphincter: a preliminary report. J Urol 138: 659-662.
30. Tokunaka S, Okamura K, Fujii H, Yachiku S (1990) The proportions of fiber types in human external urethral sphincter: Electrophoretic analysis of myosin. Urol Res 18: 341-344.
31. Bukovsky A, Copas P, Caudle MR, Cekanova M, Dassanayake T, et al. (2001) Abnormal expression of p27kip1 protein in levator ani muscle of aging women with pelvic floor disorders - A relationship to the cellular differentiation and degeneration. BMC Clin Pathol 1: 4.

32. Wells TJ (1990) Pelvic (floor) muscle exercise. J Am Geriatr Soc 38: 333-337.

33. Harvey MA (2003) Pelvic floor exercises during and after pregnancy: A systematic review of their role in preventing pelvic floor dysfunction. J Obstet Gynaecol Can 25: 487-498.

34. Jiang HH, Salcedo LB, Song B, Damaser MS (2010) Pelvic floor muscles and the external urethral sphincter have different responses to applied bladder pressure during continence. Urology 75: 1515e1-1515e7.

35. Tran C, Damaser MS (2015) The potential role of stem cells in the treatment of urinary incontinence. Ther Adv Urol 7: 22-40.

36. Eggermont M, De Wachter S, Eastham J, Gillespie J (2018) Regional structural and functional specializations in the urethra of the female rat: Evidence for complex physiological control systems. Anat Rec (Hoboken). doi: 10. 1002/ar.23795.